

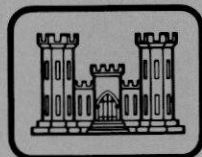
Special Report 81-3

March 1981

AN INVESTIGATION OF THE SNOW ADJACENT TO DYE-2, GREENLAND

H.T. Ueda, M.A. Goff and K.G. Nielsen

Prepared for
U.S. AIR FORCE
By



UNITED STATES ARMY
CORPS OF ENGINEERS
COLD REGIONS RESEARCH AND ENGINEERING LABORATORY
HANOVER, NEW HAMPSHIRE, U.S.A.



REPORT DOCUMENTATION PAGE		READ INSTRUCTIONS BEFORE COMPLETING FORM
1. REPORT NUMBER Special Report 81-3	2. GOVT ACCESSION NO.	3. RECIPIENT'S CATALOG NUMBER
4. TITLE (and Subtitle) AN INVESTIGATION OF THE SNOW ADJACENT TO DYE-2, GREENLAND	5. TYPE OF REPORT & PERIOD COVERED	
	6. PERFORMING ORG. REPORT NUMBER	
7. AUTHOR(s) H.T. Ueda, M.A. Goff and K.G. Nielsen	8. CONTRACT OR GRANT NUMBER(s) MIPR CS 79-162	
9. PERFORMING ORGANIZATION NAME AND ADDRESS U.S. Army Cold Regions Research and Engineering Laboratory Hanover, New Hampshire 03755	10. PROGRAM ELEMENT, PROJECT, TASK AREA & WORK UNIT NUMBERS	
11. CONTROLLING OFFICE NAME AND ADDRESS 4700th Air Defense Squadron (support) (TAC) Peterson AFB, Colorado 80914	12. REPORT DATE March 1981	
	13. NUMBER OF PAGES 27	
14. MONITORING AGENCY NAME & ADDRESS (if different from Controlling Office)	15. SECURITY CLASS. (of this report) Unclassified	
	15a. DECLASSIFICATION/DOWNGRADING SCHEDULE	
16. DISTRIBUTION STATEMENT (of this Report) Approved for public release; distribution unlimited.		
17. DISTRIBUTION STATEMENT (of the abstract entered in Block 20, if different from Report)		
18. SUPPLEMENTARY NOTES		
19. KEY WORDS (Continue on reverse side if necessary and identify by block number) DEW line Snow Snow strength		
20. ABSTRACT (Continue on reverse side if necessary and identify by block number) Snow samples from five 50-ft (15.2-m) deep holes, augered adjacent to the west side of DEW Line Station Dye-2 in Greenland, were investigated for density and unconfined compressive strength. Forty-two percent of the recovered cores were tested. Ninety-three percent of the samples tested had a length/diameter ratio greater than 2:1. The loading rate was 2 in./min (51 mm/min). Sample end-effects appeared to influence a high percentage of the failures. The heavily disturbed nature of the material is evidenced in the widely scattered values of density and strength with depth. A minimum and maximum strength value of 31 psi (0.21 MPa) and 1065 psi (7.34 MPa) respectively were obtained from a hole located 50 ft (15.2 m) from the structure. Using an approach similar to that used prior to the DYE-3 move in 1976, a safety factor exceeding 6.5 is obtained against a brittle bearing failure based on a maximum footing design load of 2000 lb/ft ² (96 kPa).		

PREFACE

This investigation was conducted by H. Ueda and M.Goff, Mechanical Engineers, Technical Services Division, U.S. Army Cold Regions Research and Engineering Laboratory; and K. Nielsen, Civil Engineering Student, Structural Research Laboratory, Technical University of Denmark. The study was prepared for and funded by the 4700th Air Defense Squadron (support) (TAC) under MIPR CS 79-162.

In addition to the authors, the following CRREL personnel participated in the project: W. Tobiasson, Program Director; A. Creatorex, field planning and preparation; C. Korhonen and B. Coutermarsh, assisting in field work. Also assisting in the field was H. Agerskov, Structural Research Laboratory, Technical University of Denmark.

W. Tobiasson, C. Korhonen, Dr. M. Mellor and F.D. Haynes of CRREL technically reviewed this report.

The contents of this report are not to be used for advertising, publication or promotional purposes. Citation of trade names does not constitute official endorsement or approval of the use of such commercial products.

AN INVESTIGATION OF THE SNOW ADJACENT TO DYE-2, GREENLAND

H.T. Ueda, M.A. Goff and K.G. Nielsen

INTRODUCTION

Two DEW Line stations were built on the Greenland Ice Cap in 1959-60. They are called DYE-2 and DYE-3 and are located near the Arctic Circle in southern Greenland (Fig. 1). The structures are quite unusual since they are founded on snow. They are supported on columns which allow the building to be periodically raised as the snow accumulates beneath them. The sub-surface column sections and supporting truss work are protected from the encroaching snow by a wooden truss enclosure (Fig. 2). The useful life of the structures is predicated on the stability of the columns and the subsurface truss work, and the action of the snow on the truss enclosure walls.

A study is currently underway to determine the remaining life of DYE-2 and to evaluate the alternatives available to extend its useful life to 1986 (Tobiasson et al. 1979, Tobiasson and Tilton 1980). As part of this study, the unconfined compressive strength of the snow adjacent to and west of DYE-2 was investigated (Fig. 3). This would be the location of a new foundation if the building is moved sideways to prolong its useful life. The results of the investigation are reported here. A similar investigation in 1976 was conducted prior to the successful sideways move of DYE-3 (Tobiasson and Bourne 1976).

The material surrounding both DYE-2 and DYE-3 has undergone approximately 20 years of various types and degrees of disturbances from

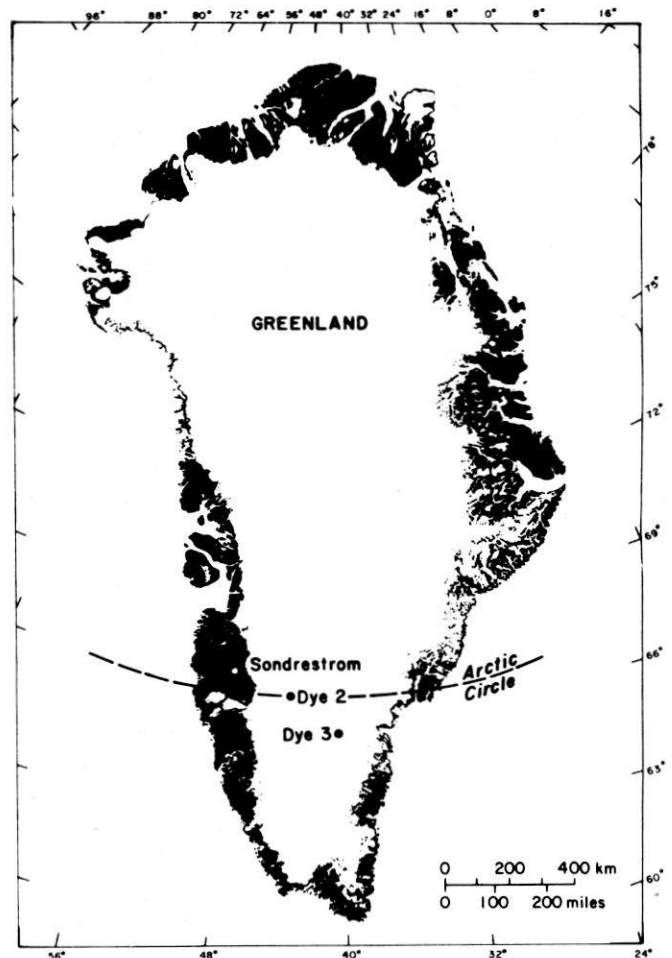


Figure 1. Location of DEW line ice cap stations DYE-2 and DYE-3.

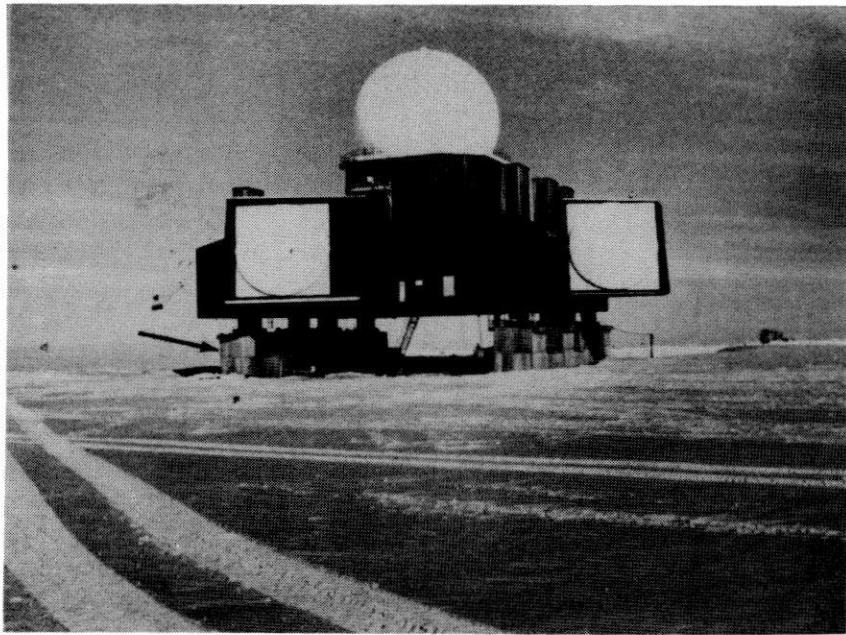


Figure 2. Surface view of the main structure at DYE-2 in 1979. Exposed portions of the truss enclosure are visible below the building (arrow).

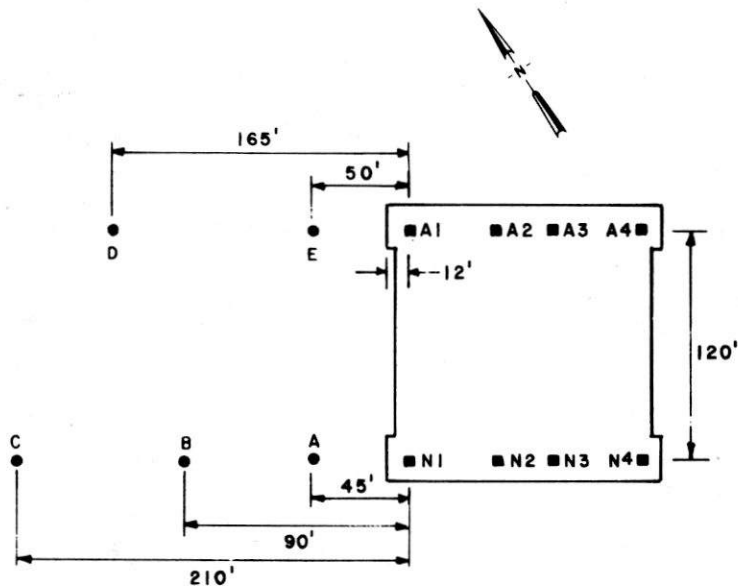


Figure 3. Sample hole locations at DYE-2.

vehicles, sleds, construction equipment and human activity. This is in addition to the normal annual snow accumulation and melt cycles experienced on the ice cap. Ice lenses up to several inches thick can be found at practically any depth below 3 ft (1 m).

These circumstances present obvious difficulties to one who is attempting to determine the mechanical or physical properties of the materi-

al with depth. The results from one hole can vary significantly from those of another hole only a few feet away. Therefore, when evaluating the results of this investigation, one must remain aware of the history behind the formation of the material. With this awareness and with a rational interpretation of the data, it should be possible to obtain a good estimate of the bearing capacity of the snow.

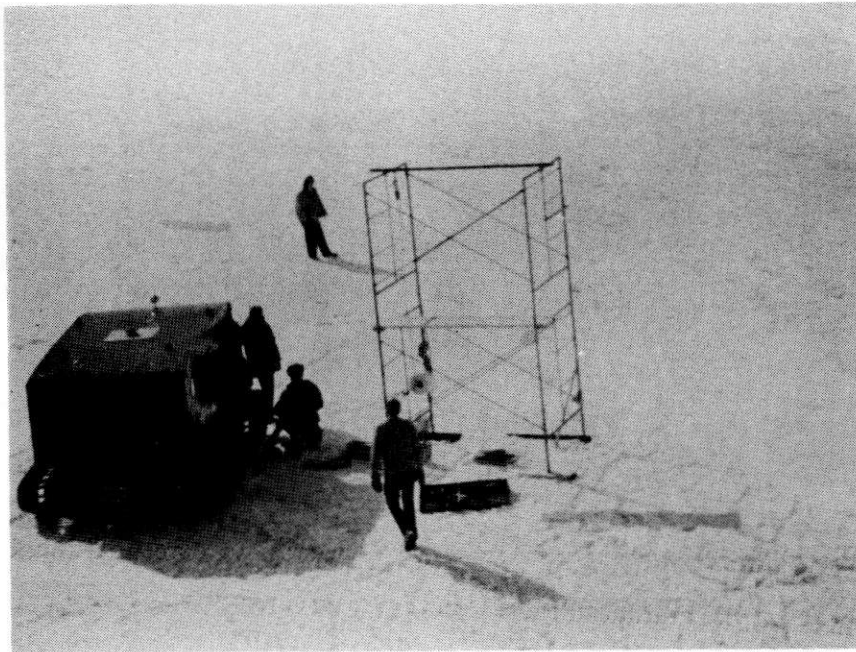


Figure 4. Core augering setup.

TEST PROCEDURE

Augering and sample preparation

During the period 26–29 July 1979, five holes were augered on the west side of DYE-2 using a CRREL 3-in. (76-mm) coring auger. Three holes were located 45 ft (13.7 m), 90 ft (27.4 m), and 210 ft (64 m) from the building along the "N" row column line. Two holes were located 50 ft (15.2 m) and 165 ft (50.3 m) from the building along the "A" row column line (Fig. 3). Each hole was augered to a depth of 50 ft (15.2 m), required an average of 39 runs, and took approximately 3.5 hr to complete. Two sections of construction scaffolding provided an overhead platform about 7 ft (2.1 m) high which permitted handling the auger extensions in 12- to 15-ft (4- to 5-m) lengths (Fig. 4).

Although the cuttings and the cores contained numerous pieces of wood and metal particles, no debris large enough to prevent further penetration was encountered until the last hole, borehole E. It took three attempts before a 50-ft (15.2-m) depth could be attained here.

A nominal 3-in. (76-mm) diameter core was obtained from most of each hole (Fig. 5). Cores varied in length from 5 to 28 in. (13 to 71 cm) and were usually in one to three pieces. Each core was numbered, its length measured, and its depth recorded before it was inserted into a polyethylene bag. After the ends were stapled,

the bag was placed in an insulated box for temporary storage during drilling. Later the cores were transported to the truss enclosure where they were stored 20 to 30 ft (6 to 9 m) below the surface at 15°F (-9°C).

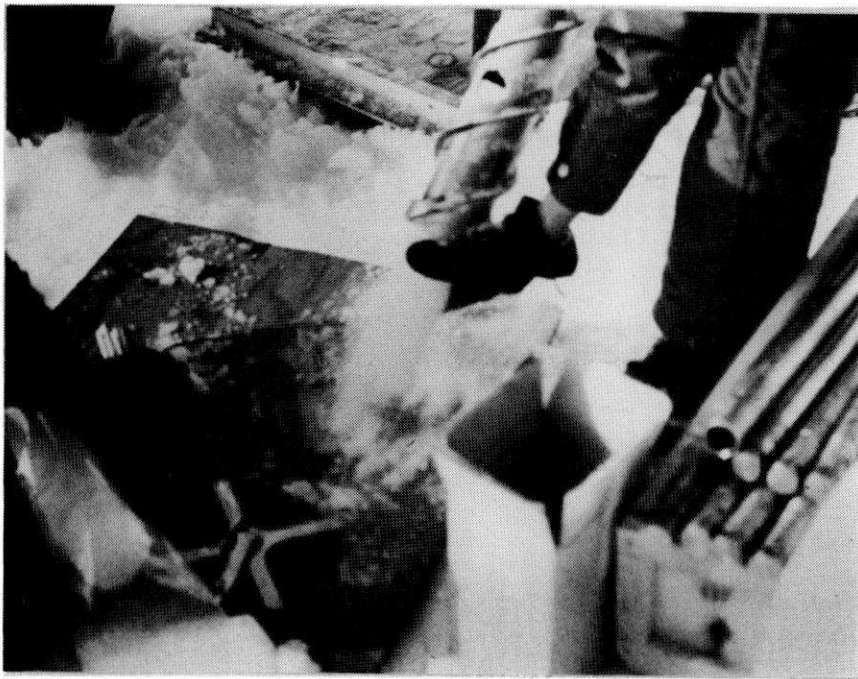
Sample preparation for unconfined compression tests began on 30 July 79. The preparation area was located on the truss enclosure stairway, about 20 ft (6 m) below the surface at 18°F (-8°C).

Usually one sample per drilling run was selected for testing. The ends of the sample were first rough-trimmed with a hand saw and a wooden miter box. Next, the sample was placed in a steel V-block where the ends were smoothed and squared. A circumferential measuring tape (Pi-tape)* and a steel rule were used to measure the diameter and length, respectively (Fig. 6).

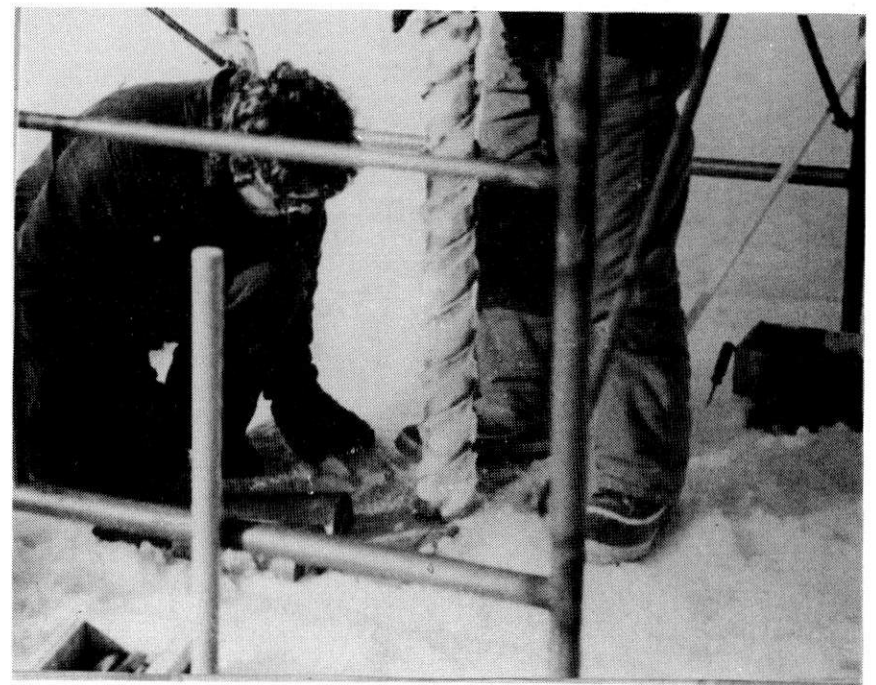
Diameters ranged from 2.88 in. (73 mm) to 3.02 in. (77 mm). Lengths varied from 5.4 in. (13.7 cm) to 9.8 in. (24.9 cm). Length-to-diameter ratios varied between 1.7:1 and 3.3:1. Ninety-three percent of the samples had a length-to-diameter ratio of 2:1 or more.

Each sample was weighed on a triple-beam balance to within 0.1 g, given a sample number, and repackaged in a plastic bag. They were then returned to the storage area. A total of 161 sam-

* Pi-Tape, Lemon Grove, California.

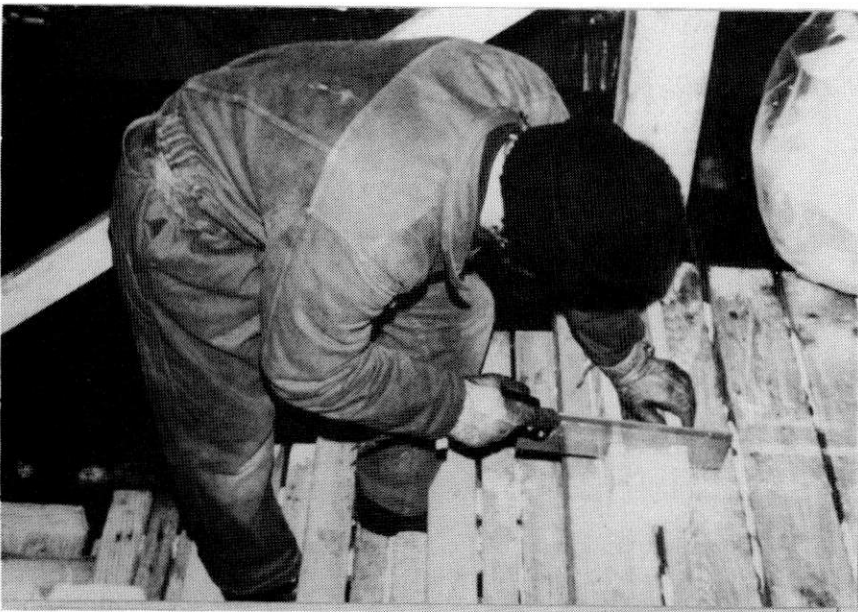


a. Removing full barrel from hole.



b. Removing core from upper end of barrel.

Figure 5. Obtaining core samples.



a. Rough squaring of sample ends in a wooden miter box.



b. Smoothing sample ends in a steel V-block.

Figure 6. Sample preparation.

ples, representing 42% of the length of recovered core, were prepared from the five holes.

Needless to say, field preparation and testing of samples do not normally lend themselves to the more refined methods available in the laboratory. Although great care was used in the preparation of the samples, there are two areas which need improvement, the shape of the sample and the finish of the ends.

It is highly unlikely that a straight cylindrical core can be obtained when augering in a non-homogeneous material such as the mixture of snow and snow ice encountered here. The auger cutting teeth tend to wander as they meet material of varying hardness. This can result in a finished sample with end surfaces not perpendicular to the true axis of the sample. The only way to overcome this condition would be to trim the sample along its length, parallel to its axis, before trimming and finishing the ends.

The finish of the end surfaces has been known to have an influence on the strength of ice (Haynes and Mellor 1977). Surface irregularities could undoubtedly have a significant effect on the strength of the sample. Obtaining the proper finish is no simple task, however, particularly in the field. We finished our ends by using a file or wood forming tool.

Equipment and test procedure

The tests were conducted in the truss enclosure about 15 ft (4.6 m) below the surface beginning on 1 Aug 79. The temperature at that level was 20°F (-6.7°C).

The samples were compressed in a modified Soiltest Model CT-405X testing machine. The installation of a $\frac{3}{4}$ -hp (1-kW), 1725-rpm electric motor and a lower ratio, mechanical drive increased the no-load platen travel rate from 0.086 in./min (2.2 mm/min) to 2 in./min (51 mm/min). The upper platen of the machine was swivel mounted. Aluminum spacers were inserted between the sample and lower platen whenever the variations in sample length exceeded the travel capacity of the machine. A $\frac{1}{16}$ -in. (1.6-mm) thick sheet of neoprene foam was placed between the sample and the upper platen. We felt this provided a better load distribution although the use of a cushion of this thickness and material may be questionable (Hawkes and Mellor 1970).

A 2000-lbf (909-kgf) or a 500-lbf (227-kgf) elec-

trical resistance strain-gage load cell was used to measure the axial force. The load cell output was recorded on a Brush Model 222 strip chart recorder with a full scale frequency response of 30 Hz. A Vishay BA-4 amplifier was used to supply the excitation to the load cells and the amplification required for the recorder.

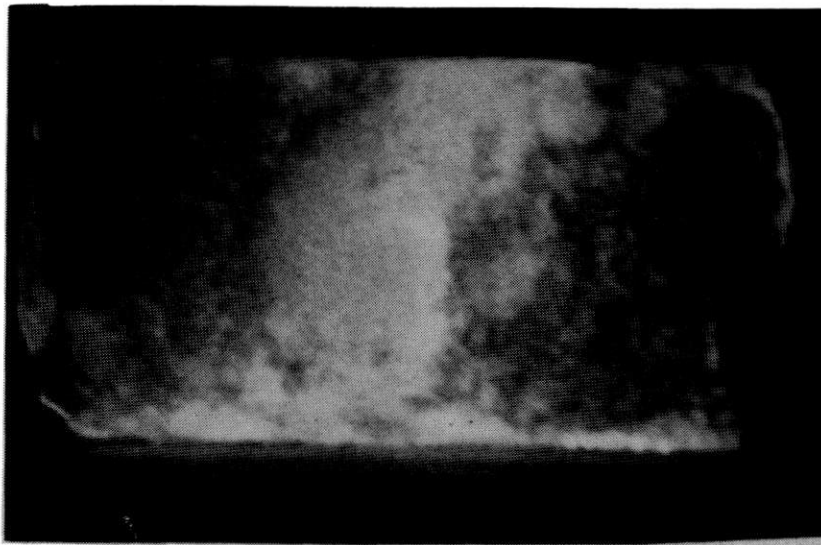
Samples were sorted according to makeup, e.g., snow, snow-ice mixtures, and glacial ice. This grouping permitted the use of the lower capacity and hence more sensitive load cell first before changing over to the higher capacity cell. Two examples of a sample with a snow-ice mixture are shown in Figures 7a and 7b. Figure 7c shows a sample heavily contaminated with what appeared to be engine oil.

No deformation or platen travel rates were measured during the tests, although several measurements were made in the laboratory with pure ice samples. With a platen speed of 2 in./min (51 mm/min) we estimate that the strain rates attained in the field tests varied from 2.5×10^{-3} to $6.0 \times 10^{-3} \text{ s}^{-1}$. At these strain rates, the failure mode should have been brittle (Mellor and Smith 1966, Hawkes and Mellor 1972). One of the reasons for selecting this rate was the data could be compared with the DYE-3 unconfined compression test results of Tobiasson and Bourne (1976).

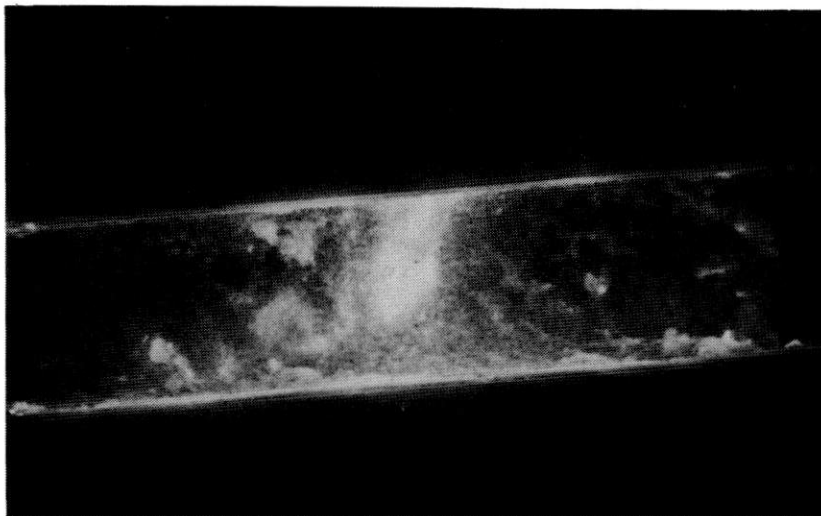
Visual observations of each failure were noted and recorded. Appendix B shows some typical failures and load-time recorder traces. Strength values were determined from the first significant peak on the load-time trace, for example, sample A23, Figure B2; sample B4, Figure B4 and sample D4, Figure B8.

In a few cases, the initial peak was followed by a slight decrease, then an increase to a value well above the initial peak load before failure. Sample A3 (Fig. B14) is an example. In such instances the initial peak was still used as the failure load. Since no strain measurements were made we assumed that any significant interruption of the load-time curve represented a potential failure strain.

The load-time trace for sample E39 (Fig. B12) was not typical. This was the strongest sample; it failed at a stress of 1065 psi (7.37 MPa) which was nearly double that of the next strongest sample. It appears that the test machine stored considerable energy before failure occurred.



a. Sample with snow/ice mixture.



b. Sample with snow/ice mixture.



c. Sample heavily contaminated with oil (left piece).

Figure 7. Typical sample photographs.

RESULTS AND DISCUSSION

About 70% of the sample failures can be classified as having some influence from end effects. Included in this category are axial cleavage failures and failures with shear planes which intersect at or near the end surfaces. Not included in the category are what we described as a shattering failure. These were normally high density, high strength samples. At failure most of the material literally shattered in an explosive manner. This is probably due to the compliance of the test machine.

The existence of any significant weak layers of granular depth hoar was not evident, at least in these holes. Although weak granular depth hoar layers exist in the natural snow at DYE-2, they are somewhat less likely to occur in the highly disturbed snow encountered here. The vehicular traffic and bulldozing activity has simply been too great during the past 15 years.

If layers such as those mentioned above did exist, they would probably be at one of the fractured surfaces resulting from the drilling of the core and therefore would have little chance of becoming part of a sample. They would have to be detected as the core is removed from the core barrel and they could crumble before being discovered. Some contaminated layers were recovered but they were mixed with relatively dense snow-ice.

Uniaxial compressive strength and density are plotted against depth in Appendix C for the five sets of samples. The proposed depth of footings associated with a sideways move are also included. These depths are based on a design footing depth of 15 to 20 ft (4.6 to 6.1 m) below the estimated 1981 snow surface (Tobiasson and Tilton 1980).

Considerable scatter is evident in all the sample sets. Samples from the most distant location, borehole C, show somewhat less scatter, as expected, since these should be the least disturbed samples. Also, as expected, samples from borehole E located 50 ft (15.2 m) from the building show the greatest scatter. The highest strength of 1065 psi (7.37 MPa) for a pure ice sample occurs 47 ft (14.3 m) deep in this hole.

It should be noted that the snow on the west side of the building, where the samples were obtained, has probably received the greatest disturbance over the years. This is the main entrance side of the building; the snow has experienced continuous traffic by large and small tracked vehicles, sleds, airplanes, runway conditioning

equipment and humans, and some contamination from petroleum products from the vehicles.

There is a sharp increase in density of the samples from the four holes closest to the building below a depth of about 15 ft (4.6 m). This presumably represents the result of activity from the life extension operation in 1976.

A comparison of sample strengths from borehole E and borehole A with data from similar locations at DYE-3 in 1976 shows that the DYE-2 snow is denser and stronger. This can be attributed to 1) the higher summer temperatures at DYE-2 which increase the densification rate and 2) the lower snow accumulation rate (about one-half that at DYE-3), which creates a denser snow for a given depth and temperature.

Below the design footing depths proposed for a sideways move, all samples displayed a strength exceeding 61 psi (0.42 MPa) except for two samples from borehole E. Samples E8 and E13 failed at 41 psi (0.28 MPa) and 31 psi (0.21 MPa) respectively. The value of 31 psi (0.21 MPa) is the minimum measured strength of the snow which will support the footings.

Prior to the sideways move of DYE-3, a considerable number of tests were conducted both in the laboratory and in-situ. These included unconfined samples and tests on model footings loaded adjacent to vertical walls to induce shear failure. From these tests we concluded that an abrupt shear failure of the snow supporting the temporary footings would not occur until the bearing load on the snow was well in excess of three times the snow's compressive strength.

The DYE-2 temporary footing geometry is expected to be identical to that used at DYE-3. If the minimum unconfined compressive strength of 31 psi (0.21 MPa) measured at DYE-2 is multiplied by the factor of three, which accounts for geometry, the minimum expected failure load equals 93 psi (0.64 MPa). Since the bearing load will be about 14 psi (0.10 MPa) the factor of safety against a bearing failure exceeds six.

If the depth of the temporary footings is increased by 4 ft (1.2 m), the 31 psi (0.21 MPa) minimum strength would not apply, and instead, a minimum strength of 61 psi (0.42 MPa) could be used. The factor of safety against a bearing failure would then exceed 13.

The above numbers apply to snow tested at a strain rate of 2.5 to $6.0 \times 10^{-3} \text{ s}^{-1}$. Because the load will be applied to the snow more gradually during the actual sideways move, the actual strain rate will be considerably less. Based on the strain behavior of the DYE-3 footings during

the sideways move there Tobiasson (pers. comm.) estimates that the strain rate will be between 10^{-8} and 10^{-9} s^{-1} .

The strength of ice decreases markedly as the strain rate decreases. However snow will densify during the slow application of a load. Densification increases the strength of snow which tends to offset the basic tendency of its component ice particles to become weaker at low rates of strain. Unfortunately the net effect (i.e., a strengthening or weakening) has not yet been determined for snow.

We have assumed that the strength of cold snow at strain rates of 10^{-8} to 10^{-9} s^{-1} is not appreciably reduced below its strength at a strain rate of 10^{-1} s^{-1} . However, since this is an assumption we also recommend that rather large factors of safety be used in the final design.

SUMMARY

There are wide variations in the density and the unconfined compressive strength of the snow adjacent to and west of DYE-2. This is not unexpected in view of the amount and the degree of disturbance that the material has undergone over the years. No weak zones or layers were detected, probably because of the constant bulldozing and vehicular activity. The disturbances have produced a material which is far stronger than the natural DYE-2 snow at the same depth.

Samples from borehole E, which is located 50 ft (15.2 m) from column A1, produced the highest and lowest strengths of 1065 psi (7.37 MPa) and 31 psi (0.21 MPa) respectively. Using the minimum value of strength found and following

the method employed for the DYE-3 analysis in 1976, we find a safety factor of six present against an abrupt bearing failure.

Assuming that sufficient measures will be taken to protect the site from abnormally warm or even wet conditions, and if footings are placed at the proposed depth of 15 to 20 ft (4.6 to 6.1 m) or lower, we conclude that the snow adjacent to DYE-2 can provide adequate support for a sideways move of the structure. If the proven success of the DYE-3 sideways move is any kind of measure, then a similar move for DYE-2 should not be considered a high risk venture, with regard to the bearing capacity of the supporting snow.

LITERATURE CITED

- Hawkes, I. and M. Mellor** (1970) Uniaxial testing in rock mechanics laboratories. *Engineering Geology*, vol. 4, no. 3.
- Hawkes, I. and M. Mellor** (1972) Deformation and fracture of ice under uniaxial stress. *Journal of Glaciology*, vol. 11, no. 61, p. 103-131.
- Haynes, F.D. and M. Mellor** (1977) Measuring the uniaxial compressive strength of ice. *Journal of Glaciology*, vol. 19, no. 81.
- Mellor, M.** (1974) A basic review of snow mechanics. *Snow Mechanics Symposium*. IAHS-AISH publication no. 114.
- Mellor, M. and J.H. Smith** (1966) Strength studies of snow. U.S. Army Cold Regions Research and Engineering Laboratory Research Report 168.
- Tobiasson, W. and R. Bourne** (1976) The feasibility of moving the DEW line ice cap stations sideways onto new foundations. CRREL contract report to the U.S. Air Force.
- Tobiasson, W., C. Korhonen and R. Redfield** (1979) Extending the useful life of DYE-2 to 1986, Part I: Preliminary findings and recommendations. CRREL Special Report 79-27.
- Tobiasson, W. and P. Tilton** (1980) Extending the useful life of DYE-2 to 1986. Part II: 1979 findings and final recommendations. CRREL Special Report 80-13.

Table A1. Density and unconfined compressive strength. Borehole A, location N1+45 ft, test temperature 20°F (-6.7°C).

Sample No.	Depth		Density		Strength	
	(ft)	(m)	(g/cm ³)	(lb/ft ³)	(psi)	(kPa)
A-1	3.4	1.04	0.646	40.3	97	671
A-2	3.0	0.91	0.660	41.2	75	515
A-3	5.1	1.55	0.616	34.5	78	541
A-4	5.7	1.74	0.593	37.0	80	548
A-5	7.6	2.32	0.538	33.6	99	682
A-6	8.2	2.50	0.539	33.6	40	277
A-7	10.8	3.29	0.719	44.9	130	893
A-8	15.4	4.70	0.780	48.7	61	420
A-9	18.3	5.58	0.723	45.1	109	752
A-10	22.0	6.71	0.872	54.4	478	3290
A-11	23.8	7.26	0.827	52.6	262	1810
A-12	24.7	7.53	0.829	51.8	362	2500
A-13	26.0	7.93	0.805	50.3	171	1180
A-14	27.2	8.29	0.880	55.0	330	2280
A-15	28.4	8.66	0.868	54.2	421	2900
A-16	29.5	8.99	0.854	53.3	475	3280
A-17	30.4	9.27	0.860	53.7	340	2350
A-18	31.3	9.54	0.878	54.8	330	2280
A-19	32.6	9.94	0.872	54.4	325	2240
A-20	33.5	10.21	0.844	52.7	173	1190
A-21	34.5	10.52	0.716	44.7	153	1050
A-22	36.6	11.16	0.659	41.2	102	704
A-23	38.1	11.62	0.878	54.8	211	1450
A-24	38.7	11.80	0.871	54.4	221	1520
A-25	40.0	12.20	0.745	46.8	193	1330
A-26	41.4	12.62	0.718	44.8	183	1260
A-27	42.4	12.93	0.711	44.4	203	1400
A-28	44.7	13.63	0.684	42.7	132	907
A-29	46.1	14.05	0.730	45.6	203	1400
A-30	49.4	15.06	0.798	49.8	193	1330

Table A2. Density and unconfined compressive strength. Borehole B, location N1+90 ft, test temperature 20°F (-6.7°C).

Sample No.	Depth		Density		Strength	
	(ft)	(m)	(g/cm ³)	(lb/ft ³)	(psi)	(kPa)
B-1	3.9	1.19	0.637	39.8	205	1410
B-2	6.0	1.83	0.642	40.1	244	1680
B-3	7.6	2.32	0.665	41.5	81	559
B-4	9.4	2.87	0.610	38.1	112	770
B-5	13.4	4.09	0.766	47.8	130	898
B-6	16.8	5.12	0.769	48.0	264	1820
B-7	18.1	5.52	0.846	52.8	330	2280
B-8	19.4	5.91	0.879	54.9	527*	3630*
B-9	20.7	6.31	0.669	41.8	153	1050
B-10	22.1	6.74	0.531	33.2	122	844
B-11	24.2	7.38	0.611	38.2	174	1200
B-12	25.6	7.80	0.850	53.1	321	2210
B-13	26.2	7.99	0.850	53.1	412	2840
B-14	29.2	8.90	0.759	47.4	213	1470
B-15	30.6	9.33	0.845	52.8	173	1200
B-16	31.1	9.48	0.720	45.0	369	2540
B-17	32.1	9.79	0.724	45.2	226	1560
B-18	32.8	10.00	0.744	46.5	173	1200
B-19	35.0	10.67	0.744	46.5	254	1750
B-20	36.1	11.01	0.657	41.0	194	1340
B-21	38.3	11.68	0.795	49.7	183	1260
B-22	39.5	12.04	0.724	45.2	133	915
B-23	40.6	12.38	0.668	41.7	123	846
B-24	42.3	12.90	0.698	43.6	234	1620
B-25	43.3	13.20	0.719	44.9	234	1610
B-26	44.8	13.66	0.807	50.4	264	1820
B-27	45.4	13.84	0.803	50.1	295	2040
B-28	46.2	14.09	0.797	49.8	326	2250
B-29	47.8	14.57	0.692	43.2	295	2030
B-30	48.8	14.88	0.774	48.3	305	2110
B-31	50.1	15.27	0.867	54.1	321	2210

* Extrapolated value (force exceeded recorder range setting, therefore the maximum value was extrapolated).

Table A3. Density and unconfined compressive strength. Borehole C, location N1+210 ft, test temperature 20°F (-6.7°C).

Sample No.	Depth		Density		Strength	
	(ft)	(m)	(g/cm ³)	(lb/ft ³)	(psi)	(kPa)
C-1	3.4	1.04	0.503	31.4	71	492
C-2	5.0	1.52	0.630	39.3	142	982
C-3	6.2	1.89	0.517	32.3	102	702
C-4	7.6	2.32	0.534	33.3	206	1420
C-5	9.3	2.84	0.534	33.4	133	914
C-6	11.6	3.54	0.619	38.6	102	704
C-7	14.9	4.54	0.842	52.6	345	2380
C-8	16.7	5.09	0.689	43.0	71	490
C-9	18.0	5.49	0.676	42.2	203	1400
C-10	19.8	6.04	0.561	35.0	92	633
C-11	21.7	6.62	0.570	35.6	72	494
C-12	23.4	7.13	0.786	49.1	286	1970
C-13	24.5	7.47	0.550	34.3	102	702
C-14	25.8	7.87	0.592	37.0	173	1190
C-15	27.5	8.38	0.606	37.8	123	847
C-16	28.7	8.75	0.551	34.4	142	980
C-17	30.4	9.27	0.552	34.5	152	1050
C-18	31.2	9.51	0.564	35.2	163	1130
C-19	32.6	9.94	0.569	35.5	71	489
C-20	33.4	10.18	0.572	35.7	122	840
C-21	35.1	10.70	0.616	38.5	274	1890
C-22	36.3	11.07	0.625	39.0	244	1680
C-23	37.8	11.52	0.607	37.9	232	1600
C-24	39.0	11.89	0.591	36.9	153	1050
C-25	40.6	12.38	0.581	36.3	92	636
C-26	42.1	12.84	0.575	35.9	82	562
C-27	43.4	13.23	0.613	38.3	193	1330
C-28	44.4	13.54	0.627	39.1	213	1470
C-29	45.9	13.99	0.624	40.0	278*	1920*
C-30	46.3	14.12	0.613	38.3	213	1470
C-31	48.1	14.66	0.607	37.9	162	1120
C-32	49.1	14.97	0.718	44.8	325	2240

* Extrapolated values

Table A4. Density and unconfined compressive strength. Borehole D, location A1+165 ft, test temperature 20°F (-6.7°C).

Sample No.	Depth		Density		Strength	
	(ft)	(m)	(g/cm ³)	(lb/ft ³)	(psi)	(kPa)
D-1	5.2	1.59	0.526	32.8	72	494
D-2	7.0	2.13	0.508	31.5	82	565
D-3	8.8	2.68	0.496	30.9	51	351
D-4	9.0	2.74	0.492	30.7	82	561
D-5	11.3	3.45	0.545	34.0	92	633
D-6	11.6	3.54	0.624	39.0	113	779
D-7	15.0	4.57	0.537	33.5	82	567
D-8	16.6	5.06	0.858	53.6	452	3120
D-9	18.6	5.67	0.748	46.7	346	2390
D-10	19.4	5.91	0.765	47.8	408	2810
D-11	21.5	6.55	0.878	54.8	377	2600
D-12	23.8	7.26	0.880	55.0	422	2910
D-13	24.3	7.41	0.871	54.4	413	2840
D-14	26.2	7.99	0.699	43.6	224	1540
D-15	30.1	9.18	0.676	42.2	173	1200
D-16	31.5	9.60	0.673	42.0	143	988
D-17	32.8	10.00	0.761	47.5	224	1550
D-18	34.3	10.46	0.699	43.7	224	1550
D-19	35.8	10.91	0.699	43.6	326	2250
D-20	37.3	11.37	0.715	44.6	305	2110
D-21	38.3	11.68	0.780	48.7	346	238
D-22	39.4	12.01	0.718	44.2	112	772
D-23	42.8	13.05	0.689	43.0	194	1340
D-24	44.3	13.51	0.867	54.1	277	1910
D-25	45.3	13.81	0.882	55.1	548*	3780*
D-26	46.2	14.09	0.794	49.6	478	3300
D-27	48.8	14.88	0.625	39.0	163	1120

* Extrapolated values

Table A5. Density and unconfined compressive strength. Borehole E, location A1+45 ft, test temperature 20°F (-6.7°C).

Sample No.	Depth		Density		Strength	
	(ft)	(m)	(g/cm ³)	(lb/ft ³)	(psi)	(kPa)
E-1	4.8	1.46	0.523	32.7	102	705
E-2	6.5	1.98	0.518	32.3	41	285
E-3	7.9	2.41	0.564	35.2	102	704
E-4	9.4	2.87	0.583	36.4	72	493
E-5	10.7	3.26	0.532	33.2	62	425
E-6	12.0	3.66	0.591	36.9	112	772
E-7	13.4	4.09	0.684	42.7	259	2030
E-8	14.3	4.36	0.627	39.1	41	280
E-9	16.0	4.88	0.709	44.3	256	1760
E-10	8.0	2.44	0.557	34.8	91	627
E-11	9.5	2.90	0.577	36.0	123	845
E-12	11.0	3.35	0.556	34.7	122	842
E-13	13.1	3.99	0.539	33.7	31	211
E-14	14.4	4.39	0.613	38.3	92	635
E-15	15.4	4.70	0.654	40.8	174	1200
E-16	17.1	5.21	0.882	55.1	92	631
E-17	20.6	6.28	0.830	51.8	122	844
E-18	22.0	6.71	0.861	53.7	301	2080
E-19	23.5	6.71	0.836	52.2	302	2080
E-20	24.5	7.47	0.895	55.9	396	2730
E-21	25.0	7.62	0.859	53.6	396	2730
E-22	26.4	8.05	0.867	54.5	300	2070
E-23	27.5	8.38	0.893	55.8	517	3570
E-24	28.4	8.66	0.880	55.0	273	1880
E-25	29.8	9.09	0.862	53.8	222	1530
E-26	30.9	9.42	0.867	54.1	321	2210
E-27	32.1	9.79	0.775	48.4	170	1170
E-28	33.3	10.15	0.873	54.5	272	1880
E-29	34.7	10.58	0.878	54.8	297	2050
E-30	36.1	11.01	0.802	50.0	220	1520
E-31	36.8	11.22	0.604	37.7	160	1100
E-32	38.1	11.62	0.836	52.2	260	1790
E-33	39.2	11.95	0.863	53.9	372	2560
E-34	40.7	12.41	0.847	52.9	482	3320
E-35	41.7	12.71	0.804	50.2	397	2740
E-36	43.5	13.26	0.805	50.2	124	855
E-37	44.6	13.60	0.849	53.0	521	3590
E-38	45.8	13.96	0.886	55.3	422	2910
E-39	46.9	14.30	0.887	55.4	1064	7340
E-40	48.2	14.70	0.839	52.4	148	1020
E-41	49.2	15.00	0.802	50.1	272	1870

APPENDIX B. TYPICAL SAMPLE FAILURES AND LOAD-TIME RECORDER TRACES.

Time progresses from right to left.

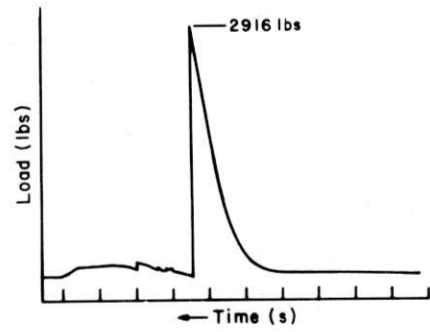
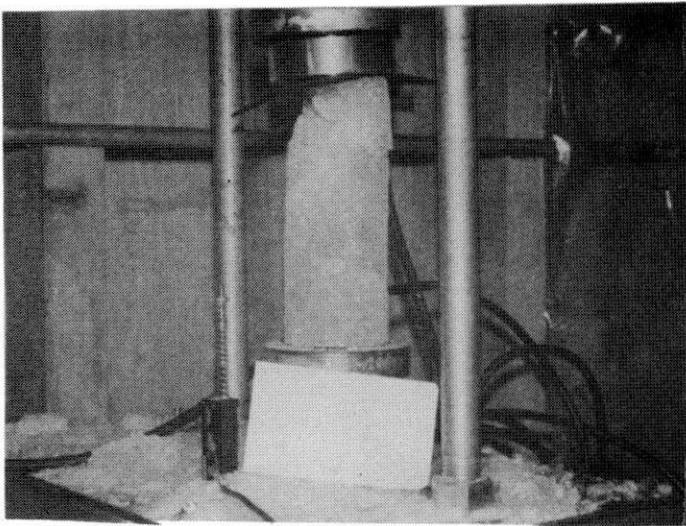


Figure B1. Sample A15 (time interval 1s).

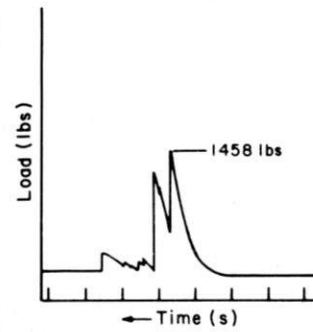
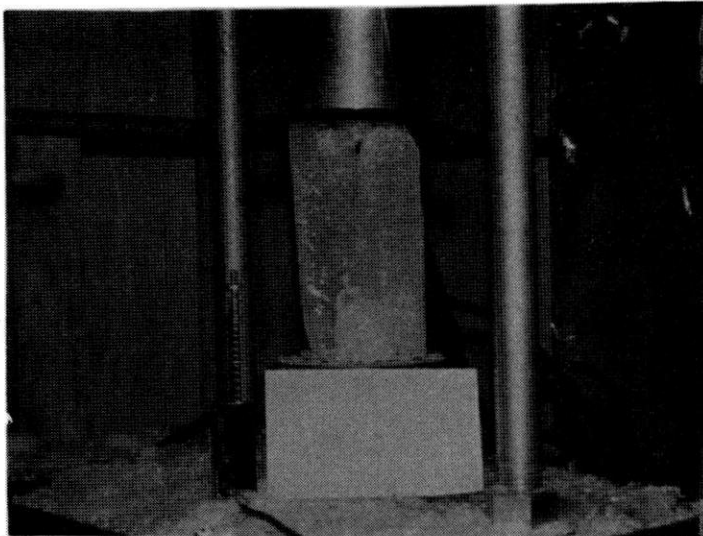


Figure B2. Sample A23 (time interval 1s).

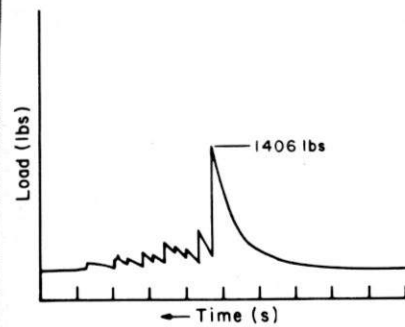
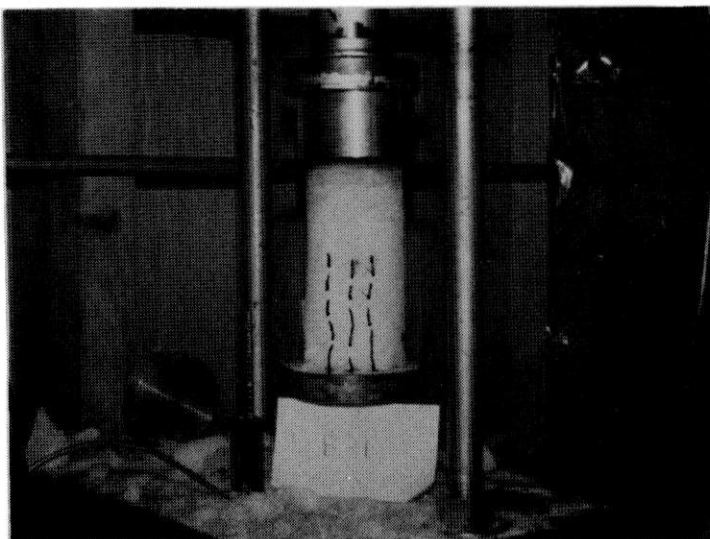


Figure B3. Sample B1, dashed lines emphasize failure mode (time interval 1s).

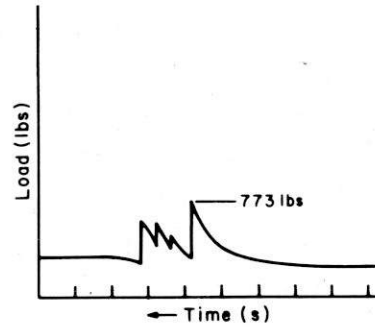
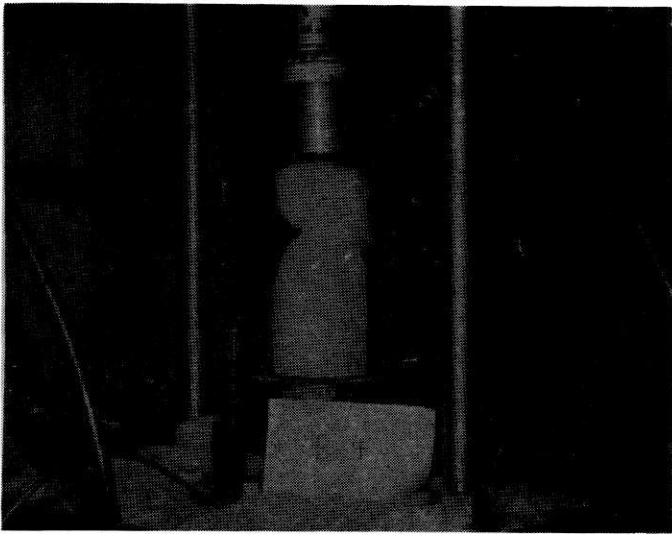


Figure B4. Sample B4 (time interval 1s).

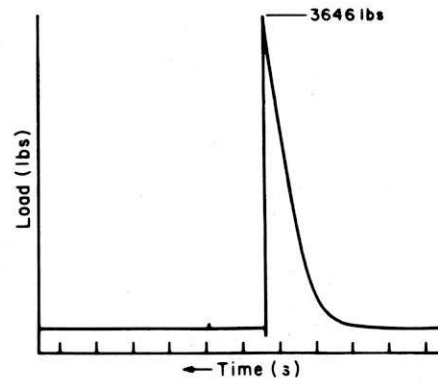
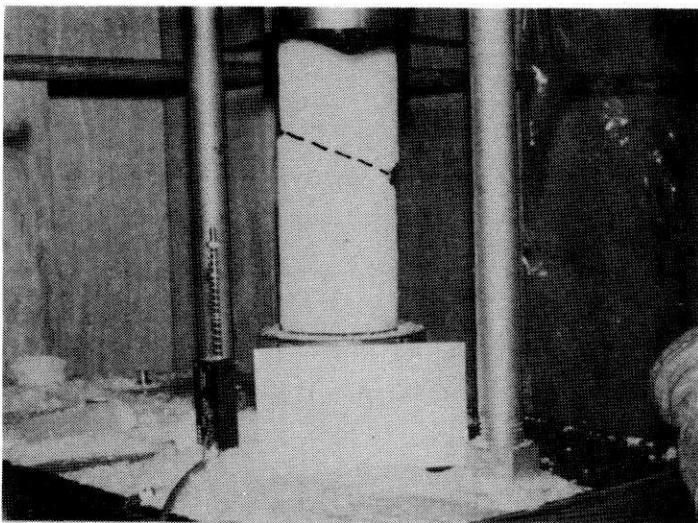


Figure B5. Sample B8, dashed line shows failure mode (time interval 1s).

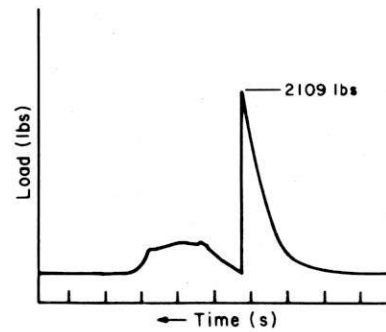
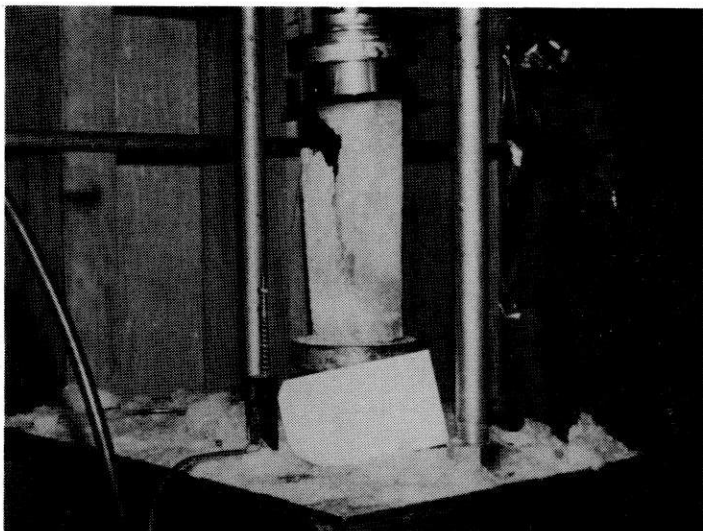


Figure B6. Sample B30 (time interval 1s).

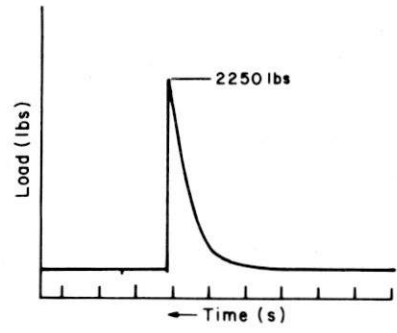
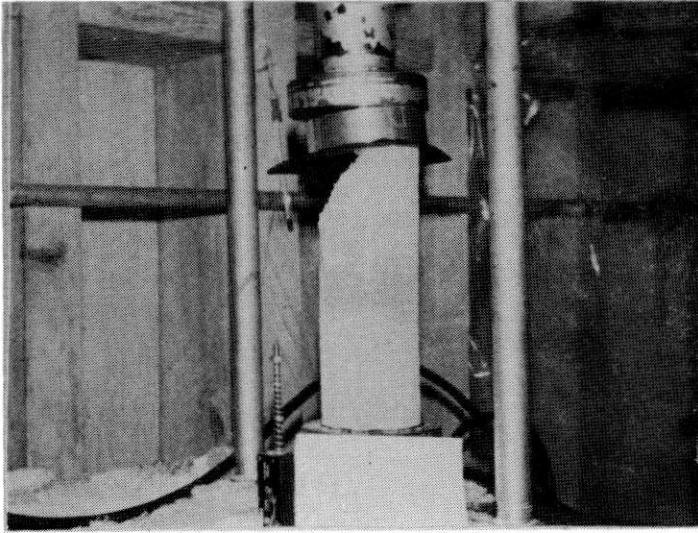


Figure B7. Sample B28 (time interval 1s).

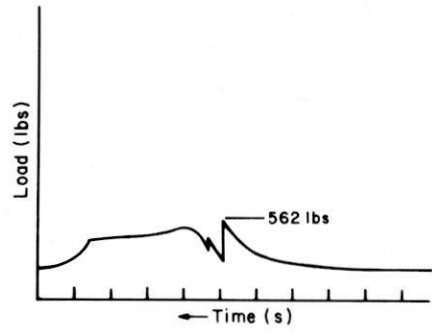
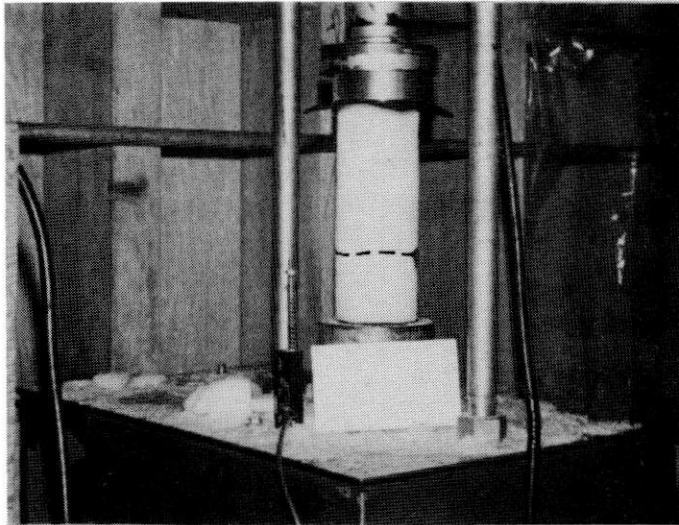


Figure B8. Sample D4, dashed line shows failure mode (time interval 1s).

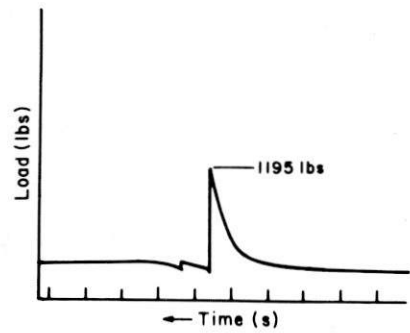
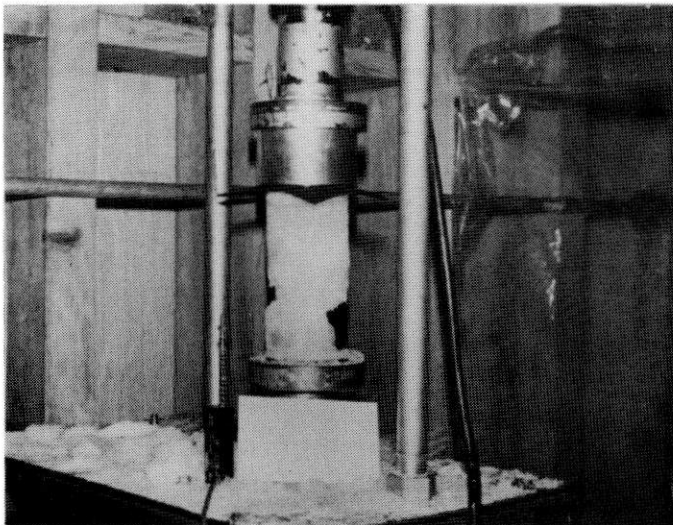


Figure B9. Sample D15 (time interval 1s).

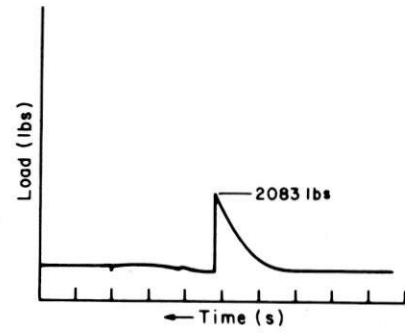
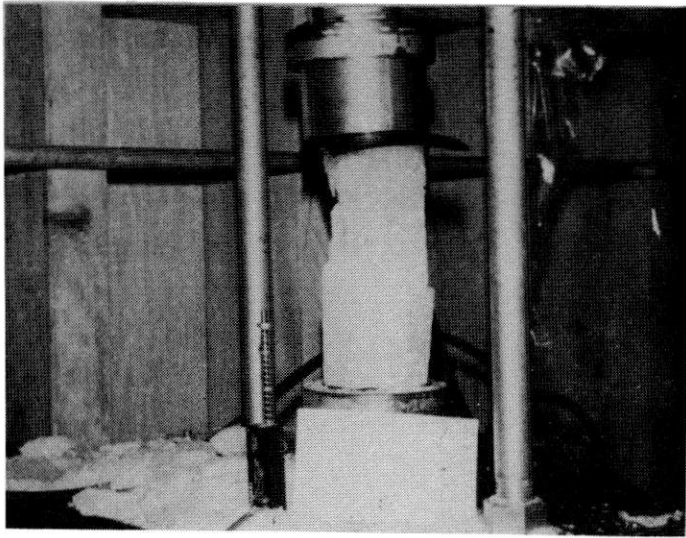


Figure B10. Sample E19 (time interval 1s).

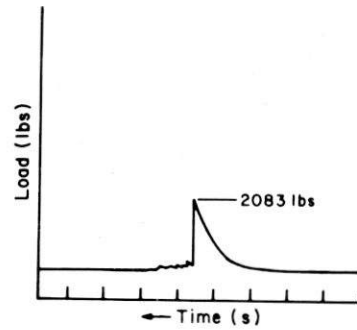
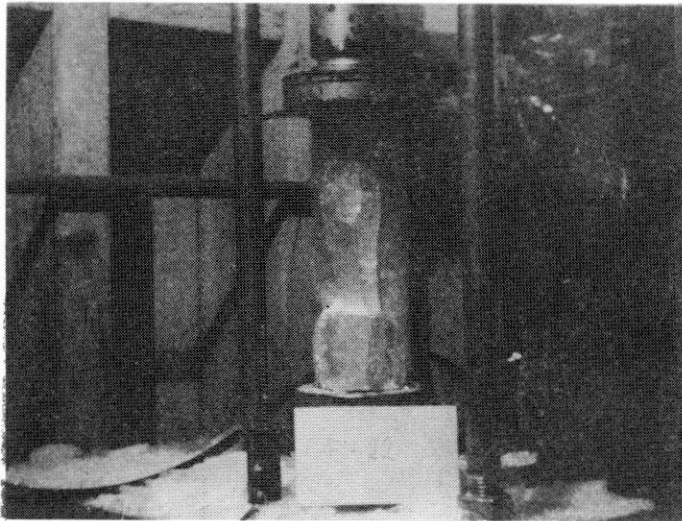


Figure B11. Sample E22 (time interval 1s).

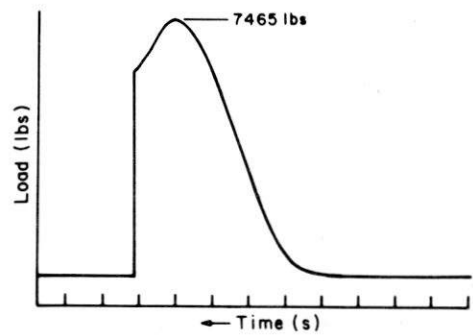


Figure B12. Sample E39 (time interval 1s).

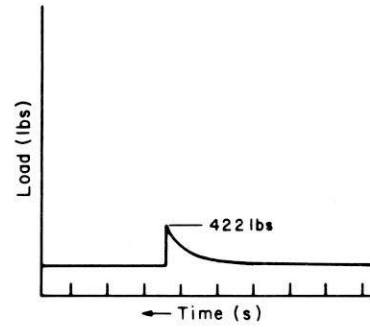
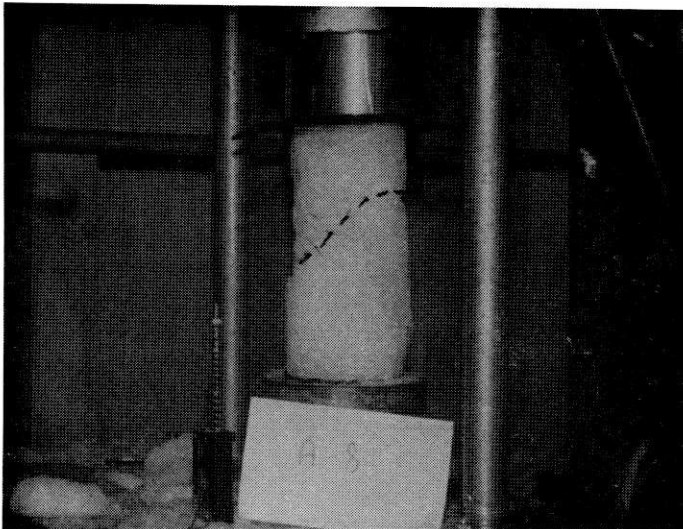


Figure B13. Sample A8, dashed line shows failure mode (time interval 1s).

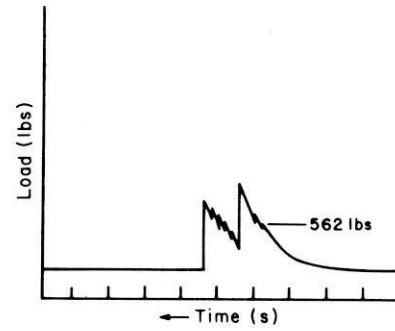
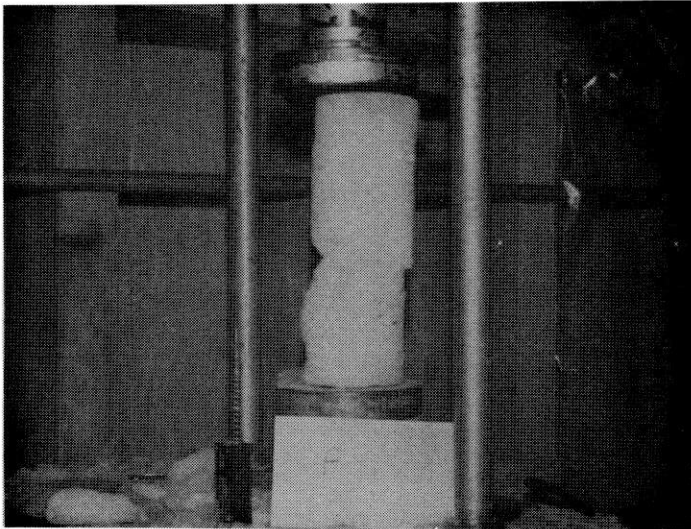
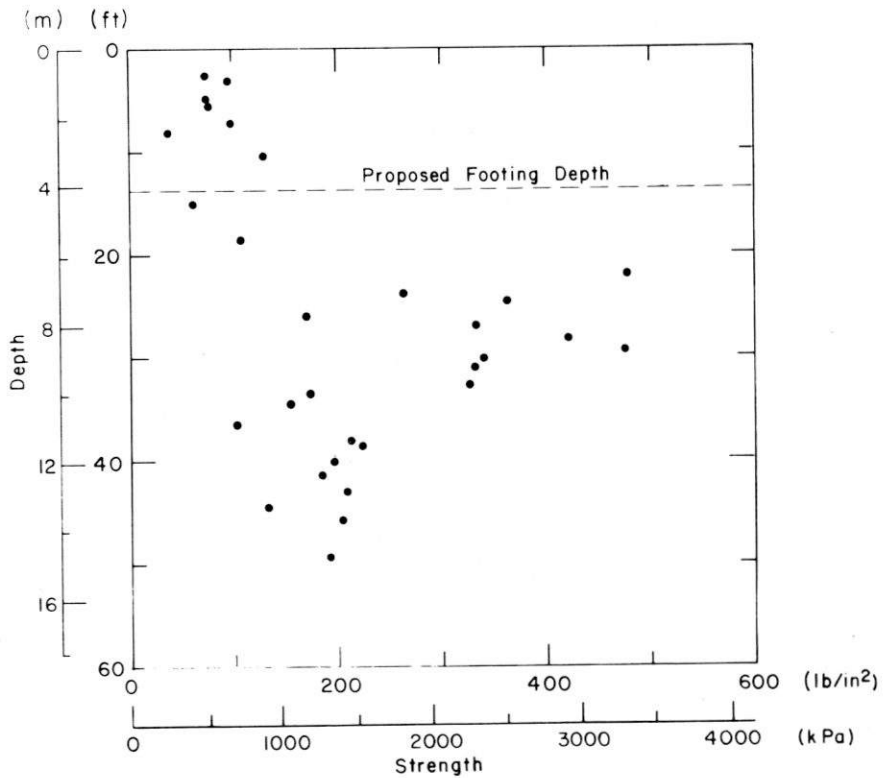
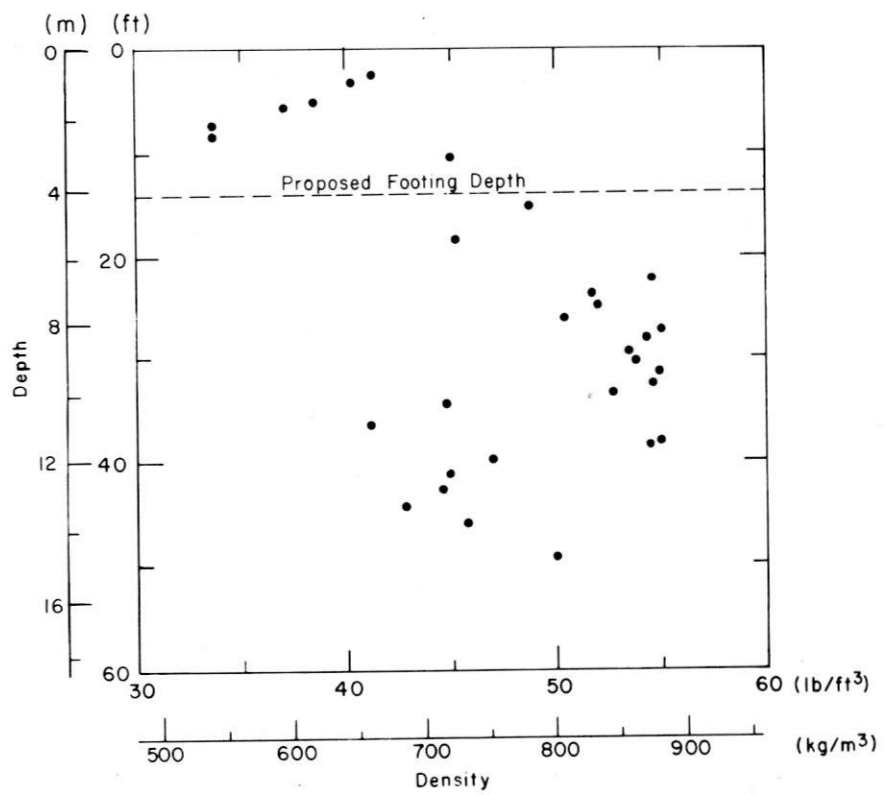


Figure B14. Sample A3 (time interval 1s).

APPENDIX C. UNCONFINED COMPRESSIVE STRENGTH AND DENSITY AS A FUNCTION OF DEPTH FOR SAMPLES FROM FIVE BOREHOLES.

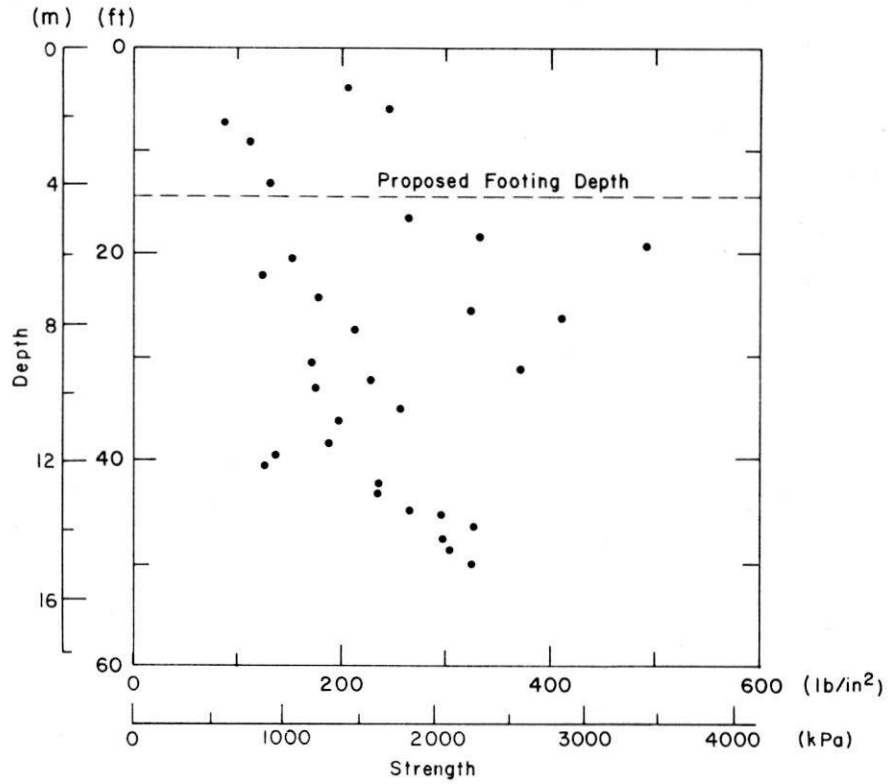


a. Strength vs depth.

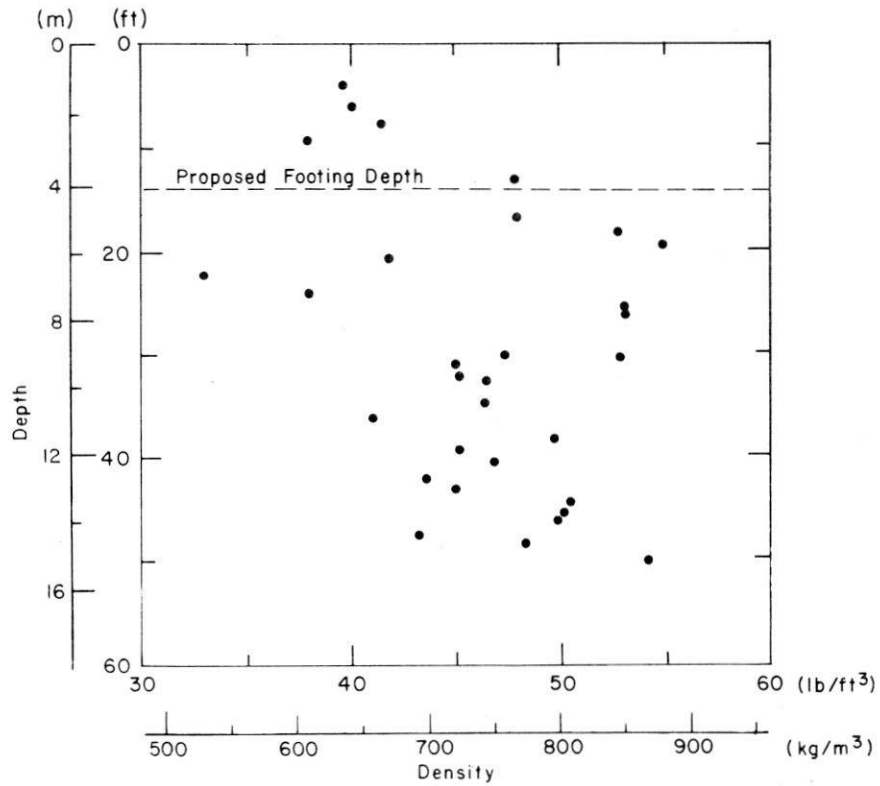


b. Density vs depth.

Figure C1. Borehole A, location N1 + 45, DYE-2, 1979.

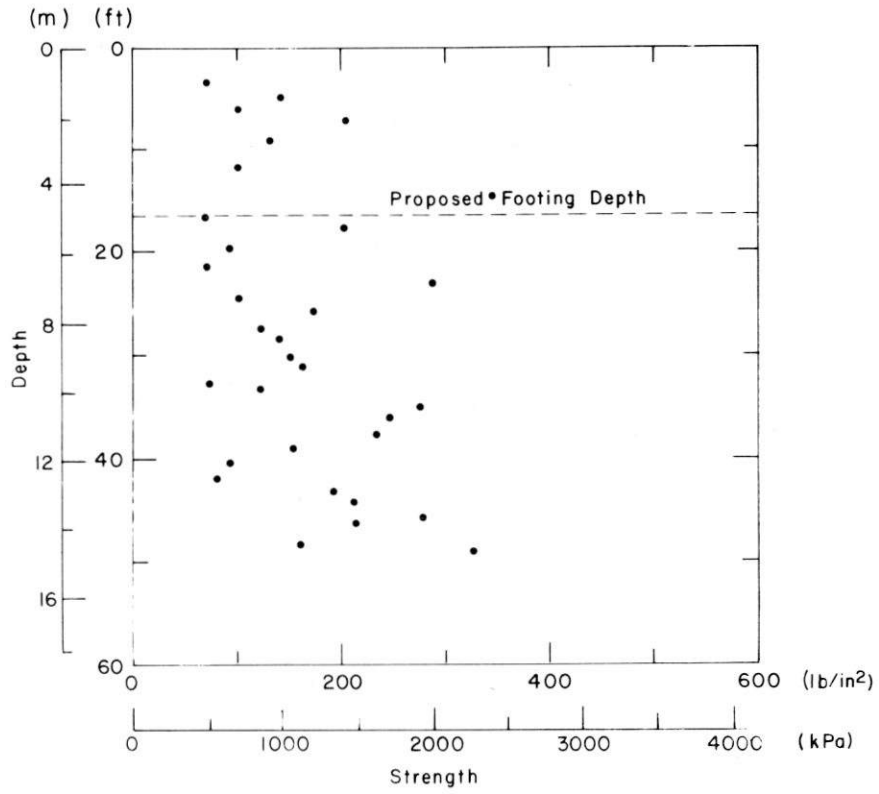


a. Strength vs depth.

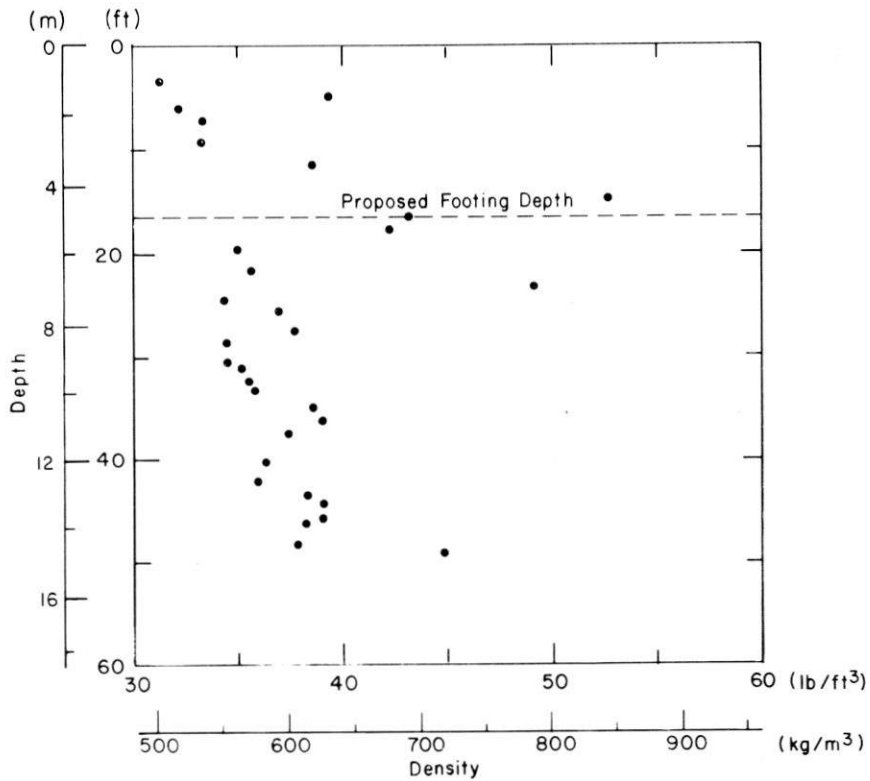


b. Density vs depth.

Figure C2. Borehole B, location N1 + 90, DYE-2, 1979.

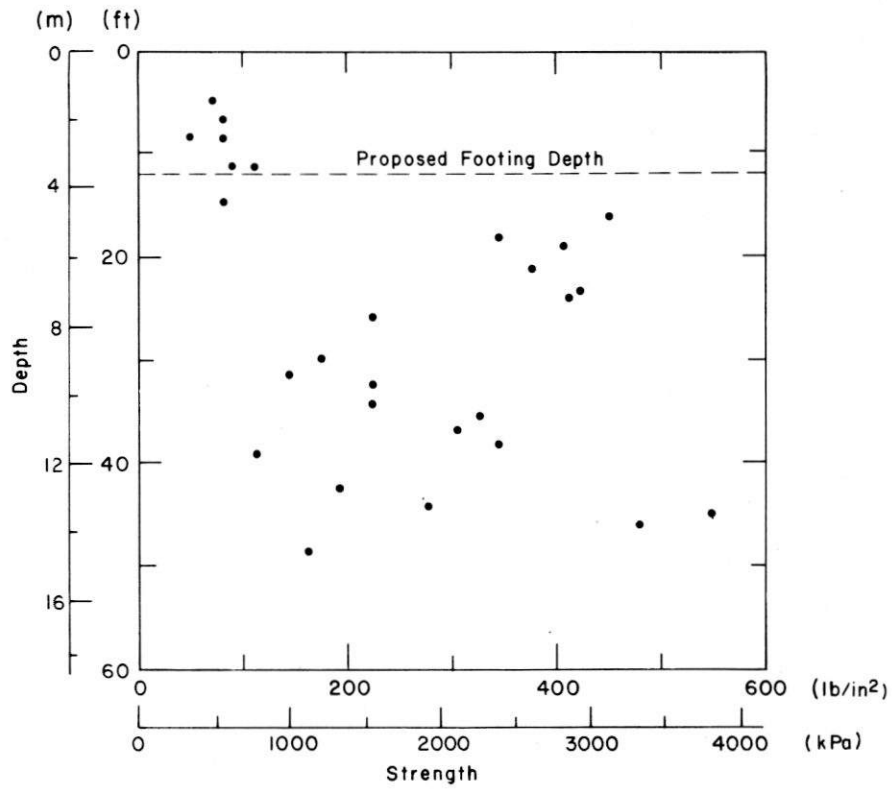


a. Strength vs depth.

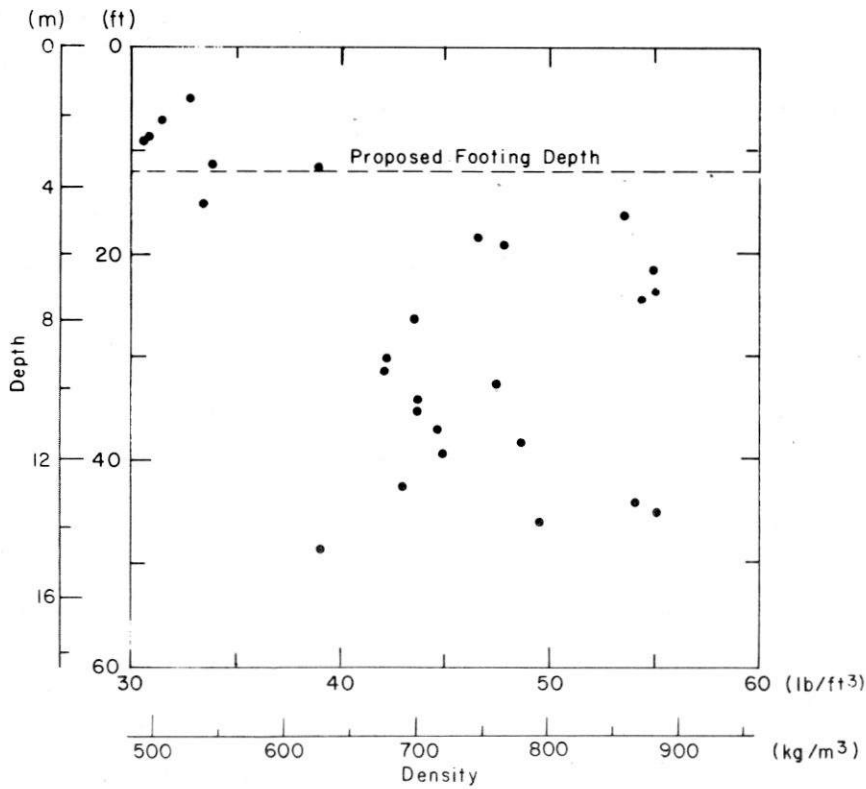


b. Density vs depth.

Figure C3. Borehole C, location N1 + 21, DYE-2, 1979.



a. Strength vs depth.



b. Density vs depth.

Figure C4. Borehole D, location A1 + 165, DYE-2, 1979.

